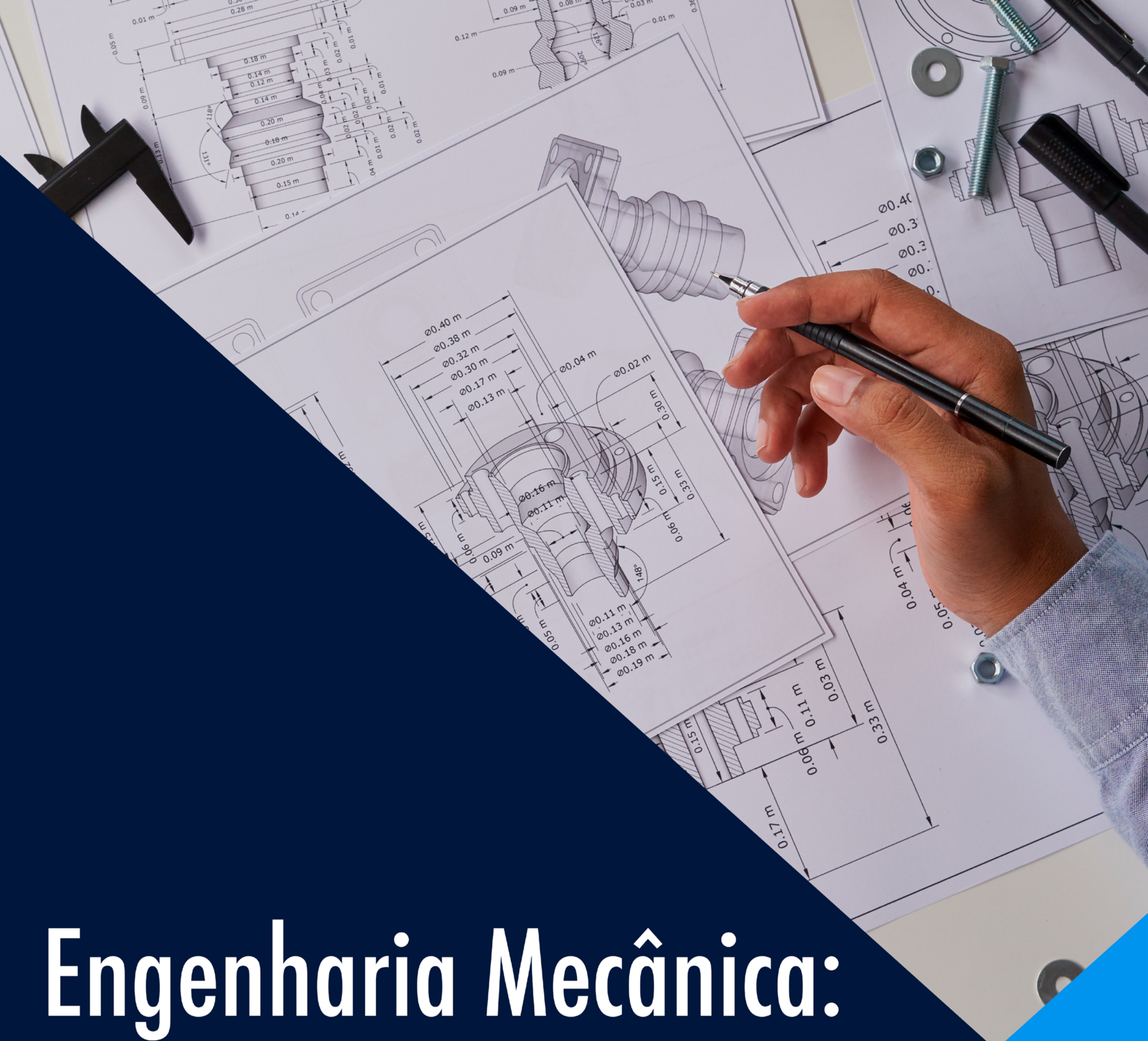

Engenharia Mecânica: Inovações Tecnológicas de Elevado Valor

Henrique Ajuz Holzmann
João Dallamuta
(Organizadores)

Atena Editora
Ano 2021

Engenharia Mecânica: Inovações Tecnológicas de Elevado Valor

Henrique Ajuz Holzmann
João Dallamuta
(Organizadores)

Atena
Editora
Ano 2021

Editora Chefe
Profª Drª Antonella Carvalho de Oliveira
Assistentes Editoriais
Natalia Oliveira
Bruno Oliveira
Flávia Roberta Barão
Bibliotecária
Janaina Ramos
Projeto Gráfico e Diagramação
Natália Sandrini de Azevedo
Camila Alves de Cremo
Luiza Alves Batista
Maria Alice Pinheiro
Imagens da Capa
Shutterstock
Edição de Arte
Luiza Alves Batista
Revisão
Os Autores

Atena Editora
Ano 2021

Atena
Editora
Ano 2021

Atena Editora
Ano 2021

Ciências Exatas e da Terra e Engenharias

Engenharia mecânica: inovações tecnológicas de elevado valor

Editora Chefe: Profª Drª Antonella Carvalho de Oliveira
Bibliotecária: Janaina Ramos
Diagramação: Maria Alice Pinheiro
Correção: Flávia Roberta Barão
Edição de Arte: Luiza Alves Batista
Revisão: Os Autores
Organizadores: Henrique Ajuz Holzmann
João Dallamuta

Dados Internacionais de Catalogação na Publicação (CIP)

E57 Engenharia mecânica: inovações tecnológicas de elevado valor / Organizadores Henrique Ajuz Holzmann, João Dallamuta. – Ponta Grossa - PR: Atena, 2021.

Formato: PDF
Requisitos de sistema: Adobe Acrobat Reader
Modo de acesso: World Wide Web
Inclui bibliografia
ISBN 978-65-5706-782-6
DOI 10.22533/at.ed.826210902

1. Engenharia mecânica. I. Holzmann, Henrique Ajuz (Organizador). II. Dallamuta, João (Organizador). III. Título.
CDD 621

Elaborado por Bibliotecária Janaina Ramos – CRB-8/9166

Atena Editora
Ponta Grossa – Paraná – Brasil
Telefone: +55 (42) 3323-5493
www.atenaeditora.com.br
contato@atenaeditora.com.br

Atena Editora
Ano 2021

DECLARAÇÃO DOS AUTORES

Os autores desta obra: 1. Atestam não possuir qualquer interesse comercial que constitua um conflito de interesses em relação ao artigo científico publicado; 2. Declaram que participaram ativamente da construção dos respectivos manuscritos, preferencialmente na: a) Concepção do estudo, e/ou aquisição de dados, e/ou análise e interpretação de dados; b) Elaboração do artigo ou revisão com vistas a tornar o material intelectualmente relevante; c) Aprovação final do manuscrito para submissão.; 3. Certificam que os artigos científicos publicados estão completamente isentos de dados e/ou resultados fraudulentos; 4. Confirmam a citação e a referência correta de todos os dados e de interpretações de dados de outras pesquisas; 5. Reconhecem terem informado todas as fontes de financiamento recebidas para a consecução da pesquisa.

Ciências Exatas e da Terra e Engenharias

Atena Editora

Ano 2021

APRESENTAÇÃO

A Engenharia Mecânica pode ser definida como o ramo da engenharia que aplica os princípios de física e ciência dos materiais para a concepção, análise, fabricação e manutenção de sistemas mecânicos. O aumento no interesse por essa área se dá principalmente pela escassez de matérias primas, a necessidade de novos materiais que possuam melhores características físicas e químicas e a necessidade de reaproveitamento dos resíduos em geral.

Nos dias atuais a busca pela redução de custos, aliado a qualidade final dos produtos é um marco na sobrevivência das empresas, reduzindo o tempo de execução e a utilização de materiais.

Neste livro são apresentados trabalho teóricos e práticos, relacionados a área de mecânica e materiais, dando um panorama dos assuntos em pesquisa atualmente. A caracterização dos materiais é de extrema importância, visto que afeta diretamente aos projetos e sua execução dentro de premissas técnicas e econômicas.

De abordagem objetiva, a obra se mostra de grande relevância para graduandos, alunos de pós-graduação, docentes e profissionais, apresentando temáticas e metodologias diversificadas, em situações reais. Sendo hoje que utilizar dos conhecimentos científicos de uma maneira eficaz e eficiente é um dos desafios dos novos engenheiros.

Boa leitura!

Henrique Ajuz Holzmann

João Dallamuta

SUMÁRIO

CAPÍTULO 2

CORRELATION BETWEEN THE TOPOGRAPHY OF THE TOOL'S WORN SURFACE AND THE RESULTING WORKPIECE ROUGHNESS IN THE MILLING PROCESS OF THE INCONEL 718

Data de aceite: 04/02/2021

Leonardo Rosa Ribeiro da Silva
Federal University of Uberlandia, School of Mechanical Engineering
Uberlândia, MG
https://orcid.org/0000-0003-2777-4500

André Rezende de Figueiredo Oliveira
Federal University of Uberlandia, School of Mechanical Engineering
Uberlândia, MG
http://lattes.cnpq.br/5032146861513670

Álisson Rocha Machado
Graduate Program in Mechanical Engineering, Pontifícia Universidade Católica do Paraná – PUC-PR
Curitiba, PR
https://orcid.org/0000-0002-5388-2954

ABSTRACT: Topographic characterization techniques are widely used for functional control of surface wear. The use of scanning electron microscopy (SEM) provides high-resolution images compared to optical systems that use the interaction of the visible light with the sample surface, that optimizes topographic characterization calculations. This work uses SEM in conjunction with image processing techniques to evaluate and correlate the topography from the wear scars at the rake face of cemented carbide tools and the resulting surface topography of an Inconel 718 workpiece in the face milling process. To study the influence of tool wear, tools with different flank wear levels (from 0.1 to 0.4 mm) artificially generated by electric discharge machining (EDM) were used. The trials were carried out under finishing, moderate and rough machining conditions, and under dry, flood and minimum lubrication (MQL) conditions. Images acquired by SEM (using secondary electrons) of the worn rake face of the cutting tools were used for calculating the topographic parameters. The results show that the topography of the wear marks on the cutting tool is related to the results of the topography of the workpieces. This innovative approach suggests that if tool wear mechanisms can be characterized by its roughness parameters, these results could be used to model the resulting roughness at the workpiece, with the reciprocal being also true.

KEYWORDS: Surface topography, Cutting forces, Tool wear, Inconel 718.

1 I INTRODUCTION

According to Popper[1], althoug phenomenologically correlations do not necessarily translate into causality, knowing the interactions between variables it is a good start for a deeper understanding of the studied phenomenon. In the machining tribosystem, those interactions are especially complex even among the other manufacturing process, as almost all variables are interdependent, leading to chaotic interactions.

The tool wear is one of the key indicators of a system machinability [2]. This variable can be measured by many methods such as interferometry [3], optical microscopy [4], scanning electron microscopy [5], and monitored using many techniques such as acoustic emission [6], vibration [7], electric power consumption [8]. The wide variety of techniques employed in the study of this phenomenon is not only the proof its complexity but also of the scientific community many doubts and little certainties about the tribological mechanisms existing in the chip-tool interface.

If analyzed properly the tool wear mechanism is like the fossil register of a machining process, and according to Astakhov [9] can be directly correlated to variables such as cutting forces and temperature, machining parameters and chemical affinity of the tool and workpiece material. The tool wear standards for continuous [10] and interrupted [11] quantify the wear mostly as a measurement of its dimensions such as the average flank wear (VB_B), maximum flank wear (VB_{Bmax}), crater wear (KT) and notch wear (VN) as main indicators. However, the analysis of the tool wear mechanism in both continuous [12] and interrupted [13] at lower [14] or higher [15] material removal rates is usually qualitative, using microscopy techniques. Although the main patterns of each wear mechanism are well known, this type of analysis leaves room for dubious interpretations and is not compatible with the scientific rigour required today for process modelling.

This paper aims at a new approach to correlate surface texture parameters at the rake face of a tool used in the milling process of Inconel 718 at different average flank wear values with the surface roughness parameters of the machined surface. This quantitative approach to the surface texture of the worn rake face of the tool leads to considerable high correlation with the roughness profile of the machined workpiece and with the cutting forces. This result demonstrates that even in a highly chaotic system such as the cutting interface if the right surface characterization parameters were chosen, correlations between the topographic characteristics of the surface could be drawn. The results also open the possibility to be the basis of new mathematical models for a more complete simulation of the surfaces interactions and resulting profiles in the machining process.

2 | EXPERIMENTAL METHODS AND MATERIALS

2.1 Workpiece Material

In this study was used as workpiece of Inconel 718 manufactured by Villares Metals S.A., under the trade name VAT718A®, with the chemical composition shown in Table 1. The Inconel was in the aged condition, having its microstructure shown in Figure 1. Figure 1a illustrates the presence of twinned grain boundaries as well as a highly oriented precipitated carbide formation. Those precipitates had his elemental composition evaluated using scanning electron microscopy and backscattered electrons (SEM-BSE) maps, as shown in Figure 1b. The precipitates are mostly composed of niobium, being probably being high hardness niobium carbides, as reported by Favero Filho, Da Silva *et al.* [5].

Ni	Cr	Fe	Nb	Mo	Ti	Al	C	Co
52,90	18,48	18,88	5,11	2,94	0,98	0,54	0,032	0,04

Table 1. Chemical composition of the Inconel 718 (% Weight).

The mechanical properties of the material were illustrated in Figure 2, with the yield and ultimate tensile strength provided by the manufacturer and the hardness of the material measured by the authors using a Vickers hardness indentation. The material bulk hardness was measured under a 100 kgf load, and the separated hardness of the matrix and the precipitated carbides under 0.5 kgf load. The matrix hardness was around 18% higher than the bulk hardness, as the microhardness have more influence in the surface oxide layer [16]. The niobium precipitate presented around two times the hardness of the bulk material and it is one of the factors that contribute to the low machinability of the material.

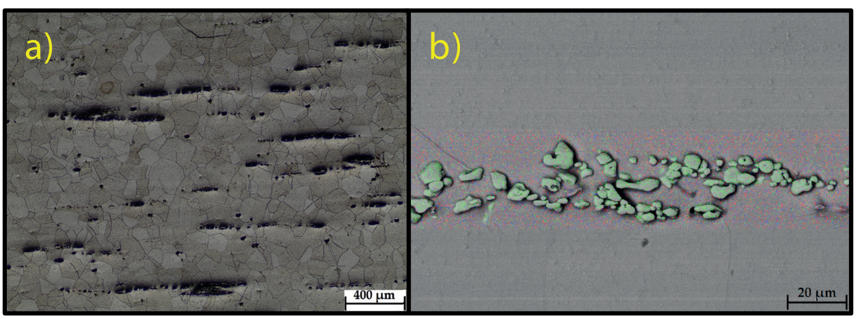

Figure 1 – (a) Optical microscopy of the microstructure of the Inconel 718 (etched with Kallings 2). (b) SEM-BSE maps using backscattered electrons of the precipitated carbides, with green for niobium, blue for chromium and red for nickel.

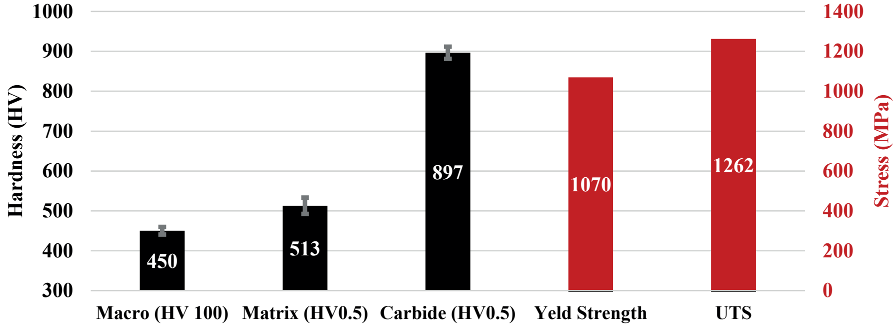

Figure 2 – Mechanical properties of the Inconel 718.

2.2 Cutting tool

For the machining tests was used a Sandvick class *"S15" (GC 1030)* cemented carbide tool *(WC-Co)*, model: *490R-140408M-PM 1030*. The inserts were coated using physical vapour deposition (PVD) with *TiAlN* and *TiN PVD*. The inserts were placed on a *Sandvick® Coromill 490* cutter body with capacity for 5 inserts and a diameter of 63 mm but only one insert was used in each trial. The tool flank wear (VBB) was artificially manufactured via electrical discharge machining, with the tool used om a negative polarity under 110 V, 40 A and pulse time of 100 µs. The tool was classified under 4 conditions as shown in the Table 2, new (no wear), type A (VBB = 0.40 ± 0.15 mm), type B (VBB = 0.70 ± 0.10 mm), type C (VBB = 1.00 ± 0.10 mm) and type D (VBB = 1.40 ± 0.150 mm).

Wear type	VB_B (mm)	Main cutting edge	Rake face
Wear Type A	0.40 ± 0.15	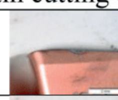	
Wear Type B	0.70 ± 0.10	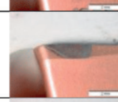	
Wear Type C	1,00 ± 0.10		
Wear Type D	1.40 ± 0.15	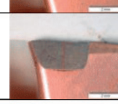	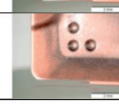

Table 2. Classification of wear produced by EDM.

2.3 Machining Tests

The machining tests were performed on a Bridgeport Discovery® 760 CNC 3-axis machining center, manufactured by ROMI, with a resolution on the x, y and z axes of 1 µm. The machining center was adapted as an open tribometer, in a similar configuration of that used by Silva, Ruzzi *et al.* [17]. Before each trial, the workpiece was pre-machined to and Rz = 2.515 ± 0.220 µm, ensuring a similar tribosystem for each repetition. The evaluated machining parameters were shown in Table 3, being classified under the finish, moderate and rough cutting conditions, for a constant cutting length of 40 mm. Each condition was performed under dry, MQL (6 bar and 50 ml/h) and flood (2.4 l/min) conditions. To ensure reproducibility were made two repetitions for each condition.

Condition	Vc (m/min)	*f* (mm/rev)	*ap* (mm)
Finish	70.0	0.10	0.25
Moderate	40.0	0.15	0.40
Rough	35.0	0.20	0.60

Table 3. Machining parameters.

2.4 Roughness parameters

After the machining trials the tools were cleaned using Nital 5% for 1 hour, and the surface texture of the worn regions were measured via scanning electron microscopy using secondary electrons (SEM-SE) in a TM3000 scanning electron microscope manufactured by Hitachi, as illustrated in Figure 3. For each tool three regions with 200x200 µm² of the rake face were taken, as the wear was mainly concentrated in this region of the tool, as illustrated in Figure 3b. This SEM-SE image were than plotted in 3D using the software MontainsMap®, using the SEM image reconstruction module, as illustrated in Figure 3c,d,e. The roughness of the machined surface was measured using a Surtronic S-100 portable surface finish & roughness measurement tester, manufactured by Taylor Hobson. To ensure reproducibility three measurements with 9.6 mm of length (Figure 4) were made for each trial.

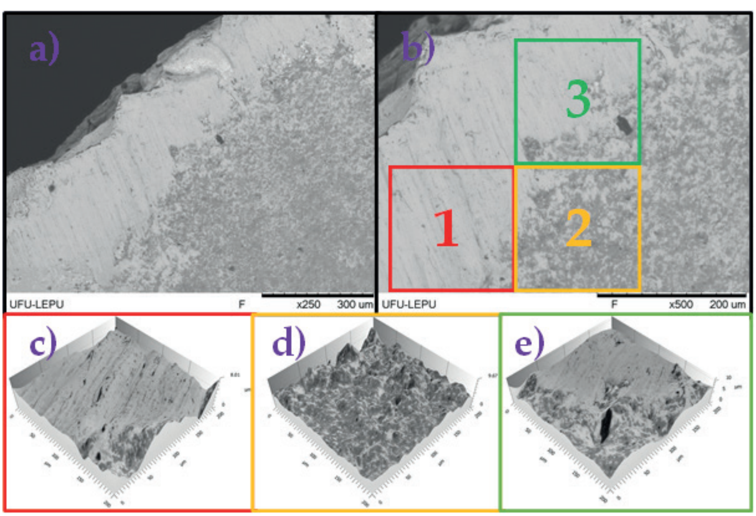

Figure 3. Creation of a 3D profile from the SEM-SE images. (a) SEM-SE image of the rake face wear; (b) Rake face wear at higher magnification and the indication of the regions transformed in 3D profiles. (c) 3D profile of the region 1; (d) 3D profile of the region 2; (e) 3D profile of the region 3.

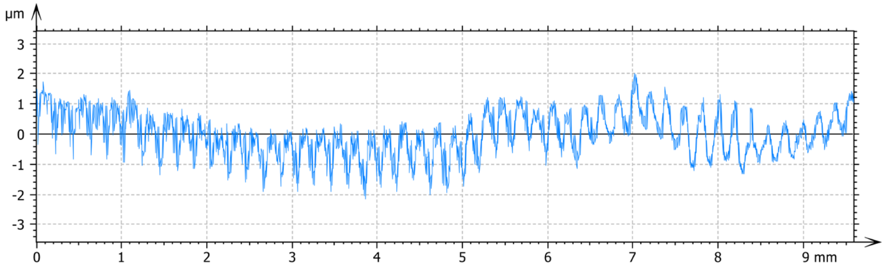

Parameters	Value	Unit
Length	9.60	mm

Figure 4. Example of a roughness profile from the workpiece after dry rough machining using a wear type A tool.

The surface texture of the tool rake surface was evaluated according to the ISO 25178 [18], and divided in amplitude, functional, spatial, hybrid, functional (volume), feature and functional (stratified surfaces) parameters, as detailed in Table 4. The roughness of the machined workpiece was evaluated according to ISO 4287 [19] in amplitude, material ratio, spacing and peak parameters, and detailed in Table 5.

Categorie	Parameter	Name	Description
Height	Sq (µm)	Root mean square	Standard deviation of the heights distance from the mean plane.
	Ssk	Skewness	Symmetry of the distribution.
	Sku	Kurtosis	Sharpness of the distribution.
	Sp (µm)	Maximum peak	Maximum value from the mean plane of the surface.
	Sv (µm)	Maximum valley	Minimum value from the mean plane of the surface.
	Sz (µm)	Maximum height	Distance between maximum and minimum height
	Sa (µm)	Arithmetical mean	Mean of the heights distance from the mean plane.
Functional	Smr (%)	Area material ratio	Percentage of cross-sectional area of the surface at a determined high.
	Smc (µm)	Inverse area material ratio	The high that gives a determined material ratio.
	Sxp (µm)	Peak extreme height	Difference of heights at the area material ratio values p% and q%.
Spatial	Sal (µm)	Auto-correlation length	Horizontal distance in the direction
	Str	Texture aspect ratio	Uuniformity of the surface texture
	Std (°)	Texture direction	Angle which the angular spectrum is the largest.
Hybrid	Sdq	Root mean square gradient	Root mean square of slopes at all points.
	Sdr (%)	Developed interfacial area ratio	Ratio between the area's additional surface added by the texture and the planar definition area.
Functional (Volume)	Vm (µm³/µm²)	Material volume	Volume of material per unit of area between a material ratio of 0% to p%.
	Vv (µm³/µm²)	Void volume	Volume of space per unit of área between a material ratio of 0% to p%.
	Vmp (µm³/µm²)	Peak material volume	Volume of material at a material ratio p%.
	Vmc (µm³/µm²)	Core void volume	Represents the difference between the void volume at a material ratio p% and q%.
	Vvc (µm³/µm²)	Core material volume	Represents the difference between the material volume at a material ratio p% and q%.
	Vvv (µm³/µm²)	Dale void volume	Represents the void volume of dale at an area material ratio p%.
Feature	Spd (1/µm²)	Density of peaks	Number of peaks per unit of area.
	Spc (1/µm)	Aritimetic mean peak curvature	Arithmetic mean of the curvature of the peaks.
Functional (Stratified Surfaces)	Sk (µm)	Core roughness depth	Difference of heights at material ratio values 0% and 100% on the equivalent line.
	Spk (µm)	Reduced peak height	Mean height of peaks above the core surface
	Svk (µm)	Reduced valley depth	Mean depth of valleys below the core surface
	Smr1 (%)	Peak material portion	Percentage of surface at the intersection of the core surface and the peak height.
	Smr2 (%)	Valley material portion	Percentage of surface at the intersection of the core surface and the valley height.

Table 5. Surface roughness parameters of the workpiece according to ISO 4287 [19].

Categorie	Parameter	Name	Description
Amplitude	Rp (µm)	Maximum peak height	Maximum height of the profile above the mean line.
	Rv (µm)	Maximum valley height	Maximum depth of the profile above the mean line.
	Rz (µm)	Ten-point height	Difference in high between the average of the five highest peaks and five lowest valleys.
	Rc (µm)	Mean height of profile	Average values of the distance between the peaks and neighbouring valleys.
	Rt (µm)	Maximum profile height	Vertical distance between the highest peak and lowest valley.
	Ra (µm)	Arithmetic average height	Arithmetic average of the profile.
	Rq (µm)	Root mean square roughness	Standard deviation of the surface heights.
	Rsk	Skewness	Profile symmetry.
	Rku	Kurtosis	Profile sharpness.
Material Ratio	Rmr (%)	Length ratio	Ratio between the length of the profile elements in relation to a material ratio c%.
	Rdc (µm)	Profile section height difference	Height difference in section height, matching the two material ratios c% and q%.
Spacing	RSm (mm)	Mean width	Mean of the length of profile elements,
	Rdq (°)	Root mean square slope	Root mean square for the local slope within the sampling length.
Peak	RPc (1/mm)	Peak count	Number of roughness profile peaks per unit of length.

To evaluate the correlations is proposed the representation shown in Table 6. The average values of iartificially manufactured tool wear (Table 4) will be correlated using the Pearson index with the roughness parameters of the workpiece (Table 5), in a similar way that was proposed by Da Silva, Da Silva *et al.* [20]. The direct correlations will have the corresponding cell coloured in green and the inverse correlation in red. The color palette will be directly related to the strength of the correlation, with deeper and lighter colors meaning correlations closer to, respectively, 100% and 0%. The overall percentual correlation of a parameter class will also be presented in a cell at the opposing side of the table.

	Roughness parameters of the machined workpiece / cutting force	Parameter class β		
Roughness parameters of the rake face of the tool		Parameter X	Parameter Y	
Parameter class α	Parameter A	Stronger direct Pearson's correlation between A and X	Weaker inverse Pearson's correlation between A and Y	Average correlation for the parameter class α
	Parameter B	Weaker direct Pearson's correlation between B and X	Stronger inverse Pearson's correlation between B and Y	
		Average correlation for the parameter class β		

Table 6. Example of how the correlations will be presented for the average values of each input variable.

3 I RESULTS AND DISCUSSION

3.1 Correlations in relation to the tool wear condition

Table 7 presents the correlations between the amplitude parameters of the machined surface (Figure 4) and the roughness parameters of the rake face of the tool (Figure 3) in relation to the average values for each of the different tool wear conditions (Table 2). In general, the workpiece amplitude surface roughness parameters resulted in above 70% correlations with the worn tool roughness parameters. This relatively high correlation can be explained by the influence of the main cutting-edge wear on the stresses and strains at the cutting interface, as similarly reported by Musfirah, Ghani *et al.* [21]. An even greater discrepancy was found between the roughness of the rake face of the tool with the average correlation of the *Rsk* and *Rku* (52.5%) and the other amplitude parameters (77.5%).

The amplitude parameters of the workpiece and height parameters of the tool presented an overall 72% correlation, with most parameters presenting above 90% correlation except for the skewness and kurtosis of each surface. These results indicate that parameters more focused on the actual height of peaks and valleys are more suited for modelling the relations between the wear at the rake face of the tool and the workpiece surface roughness than the third (skewness) and fourth (kurtosis) central moments of the distribution, with are more related with the dispersion of the profile amplitude.

In general, the spatial and functional (stratified surfaces) were the only tool wear surface roughness parameters with lower than 70% correlation with the amplitude of the workpiece profile. This can be explained by the fact that the wear at the main cutting edge is directly related with the contact pressures at the cutting interface [22] increasing the region in with the real contact area is equal to the apparent. As the spatial parameters are related with the texture direction and the functional (stratified surfaces) with the bearing area and increasing real contact area will make the differences regarding these classes of parameters irrelevant in relation to the material flow.

The highest correlations (above 80%) were found for the hybrid and functional volume classes of surface roughness parameters for worn rake face of the tool. As the increased tool wear at the main cutting-edge has a known relation with higher cutting pressures [22], and increase in the volume of the wear patterns of the tool was already expected to be related with an increased amplitude of the roughness profile at the workpiece. As the hybrid parameters are correlated with the uniformity of the workpiece, the higher contact pressured and overall harsher cutting conditions caused by the increased tool wear (Table 2) lead to more non-uniform wear of the rake surface, with can cause unbalance in the chip formation and consequently higher amplitude of the roughness profile at the workpiece.

ISO 25178	ISO 4287	Amplitude									
	Parameter	Rp (µm)	Rv (µm)	Rz (µm)	Rc (µm)	Rt (µm)	Ra (µm)	Rq (µm)	Rsk	Rku	
Height	Sq (µm)	96.5%	90.6%	96.5%	92.9%	87.5%	97.3%	97.3%	-51.4%	37.8%	72.0%
	Ssk	34.6%	-19.5%	1.6%	-19.1%	-18.3%	21.5%	15.3%	68.8%	-71.9%	
	Sku	-78.1%	-52.9%	-65.1%	-57.1%	-55.7%	-69.9%	-67.9%	14.1%	5.1%	
	Sp (µm)	96.2%	93.5%	98.2%	95.1%	90.4%	97.9%	98.3%	-56.2%	44.2%	
	Sv (µm)	95.7%	93.8%	98.2%	95.4%	90.1%	98.0%	98.4%	-56.4%	44.8%	
	Sz (µm)	96.0%	93.7%	98.2%	95.3%	90.3%	98.0%	98.4%	-56.3%	44.5%	
	Sa (µm)	96.8%	89.8%	96.1%	92.1%	86.9%	97.3%	97.2%	-49.9%	36.2%	
Functional	Smr (%)	-25.6%	-58.3%	-47.4%	-54.1%	-69.4%	-27.6%	-34.3%	81.1%	-81.9%	73.4%
	Smc (µm)	96.8%	89.0%	95.6%	91.4%	86.5%	96.8%	96.6%	-49.1%	35.0%	
	Sxp (µm)	91.5%	93.5%	96.3%	96.2%	89.1%	94.8%	95.5%	-60.6%	47.1%	
Spatial	Sal (µm)	66.1%	30.5%	46.0%	33.1%	19.2%	65.0%	59.3%	28.0%	-33.6%	55.2%
	Str	-65.9%	-94.2%	-86.4%	-95.2%	-90.8%	-74.9%	-78.9%	88.8%	-80.4%	
	Std (°)	-25.2%	-41.6%	-36.6%	-38.6%	-55.4%	-21.3%	-26.2%	56.7%	-53.5%	
Hybrid	Sdq	77.8%	92.0%	89.9%	93.7%	94.6%	79.7%	82.9%	-79.2%	65.3%	84.3%
	Sdr (%)	75.7%	92.9%	89.6%	93.7%	96.1%	78.1%	81.9%	-82.9%	71.0%	
Functional (Volume)	Vm (µm³/µm²)	99.1%	87.1%	95.3%	88.6%	84.2%	98.7%	98.0%	-42.1%	30.4%	82.1%
	Vv (µm³/µm²)	96.9%	89.0%	95.6%	91.4%	86.4%	96.9%	96.7%	-48.8%	34.8%	
	Vmp (µm³/µm²)	99.1%	87.1%	95.3%	88.6%	84.2%	98.7%	98.0%	-42.1%	30.4%	
	Vmc (µm³/µm²)	95.5%	90.3%	95.9%	93.0%	87.4%	96.3%	96.3%	-52.5%	38.0%	
	Vvc (µm³/µm²)	97.0%	88.2%	95.2%	90.6%	85.8%	96.7%	96.4%	-47.5%	33.4%	
	Vvv (µm³/µm²)	92.1%	94.4%	97.1%	96.6%	89.9%	95.6%	96.4%	-61.1%	48.6%	
Feature	Spd (1/µm²)	-83.5%	-74.5%	-81.0%	-79.3%	-64.9%	-86.9%	-85.1%	32.8%	-17.9%	76.8%
	Spc (1/µm)	-84.7%	-95.1%	-94.6%	-92.2%	-91.7%	-91.0%	-93.2%	67.0%	-67.1%	
Functional (Stratified Surfaces)	Sk (µm)	66.2%	83.6%	79.9%	86.4%	87.5%	67.5%	71.1%	-79.5%	63.1%	62.0%
	Spk (µm)	63.5%	81.4%	77.3%	86.4%	81.7%	66.5%	69.4%	-76.7%	56.8%	
	Svk (µm)	88.3%	98.1%	98.0%	97.5%	99.1%	91.0%	93.8%	-74.8%	66.7%	
	Smr1 (%)	-23.3%	-44.7%	-37.8%	-40.5%	-58.2%	-21.0%	-26.6%	62.8%	-62.7%	
	Smr2 (%)	20.0%	31.5%	28.1%	37.2%	39.8%	15.8%	18.6%	-46.3%	25.4%	
		72.0%									

Table 7. Correlation between the rake face of the worn tool roughness parameters according to ISO 25178 and the workpiece amplitude surface roughness parameters according to ISO 4287 in relation to the average values for tool wear condition.

The feature parameters of the rake face of the tool resulted in inverse correlation with the amplitude of the roughness profile at the workpiece as the tool wear increases. The inverse correlation between the number of peaks per area (*Spd*) and peak curvature (Spc) at the rake face with the roughness of the workpiece can be explained by the higher contact pressured in the cutting interface, with probably levelled the peaks reducing its number per area and curvature. In relation to the functional parameters only the (*Smr*) resulted in a poor correlation with the amplitude of the roughness profile at the workpiece (53.3%), as it describes the bearing area at the rake face, with has lower significance at higher contact pressures, leading to a poor correlation with the workpiece roughness as the tool wear increases.

	ISO 4287	Material Ratio		Spacing		Peak	
ISO 25178	Parameter	Rmr (%)	Rdc (µm)	RSm (mm)	Rdq (°)	RPc (1/mm)	
Height	Sq (µm)	-95.8%	96.8%	41.4%	97.8%	-39.9%	
	Ssk	-32.6%	27.7%	-72.3%	0.3%	73.0%	
	Sku	81.2%	-71.2%	-9.5%	-65.7%	4.9%	
	Sp (µm)	-95.6%	96.8%	43.2%	99.1%	-41.8%	66.1%
	Sv (µm)	-94.7%	97.0%	44.5%	99.3%	-43.4%	
	Sz (µm)	-95.2%	96.9%	43.9%	99.3%	-42.6%	
	Sa (µm)	-96.2%	96.8%	39.8%	97.4%	-38.2%	
Functional	Smr (%)	37.7%	-18.8%	-34.3%	-41.8%	27.5%	
	Smc (µm)	-96.4%	96.3%	38.9%	96.8%	-37.1%	61.2%
	Sxp (µm)	-90.1%	93.7%	55.2%	98.4%	-54.3%	
Spatial	Sal (µm)	-55.4%	71.5%	-11.5%	49.8%	6.7%	
	Str	66.5%	-70.4%	-78.3%	-87.9%	77.5%	45.0%
	Std (°)	38.7%	-14.1%	-12.6%	-30.7%	4.2%	
Hybrid	Sdq	-83.1%	75.3%	59.8%	89.6%	-55.2%	71.9%
	Sdr (%)	-81.5%	73.0%	58.9%	88.6%	-54.2%	
Functional (Volume)	Vm (µm³/µm²)	-98.0%	98.7%	28.8%	96.0%	-27.5%	
	Vv (µm³/µm²)	-96.5%	96.4%	38.6%	96.8%	-36.8%	
	Vmp (µm³/µm²)	-98.0%	98.7%	28.8%	96.0%	-27.5%	73.0%
	Vmc (µm³/µm²)	-95.0%	95.7%	44.0%	97.4%	-42.3%	
	Vvc (µm³/µm²)	-96.8%	96.3%	37.0%	96.3%	-35.1%	
	Vvv (µm³/µm²)	-90.6%	94.4%	53.6%	99.0%	-52.9%	
Feature	Spd (1/µm²)	77.0%	-89.3%	-48.2%	-85.9%	50.3%	69.1%
	Spc (1/µm)	83.9%	-87.7%	-37.5%	-93.3%	37.6%	
Functional (Stratified Surfaces)	Sk (µm)	-72.8%	62.8%	65.3%	80.0%	-59.9%	
	Spk (µm)	-67.2%	63.1%	78.6%	79.9%	-74.8%	
	Svk (µm)	-91.7%	86.9%	46.2%	96.6%	-43.0%	53.3%
	Smr1 (%)	36.6%	-13.1%	-14.2%	-31.4%	6.2%	
	Smr2 (%)	-29.4%	12.5%	49.2%	28.9%	-41.9%	
		76.2%		61%		40.6%	

Table 8. Correlation between the rake face of the worn tool roughness parameters according to ISO 25178 and the workpiece amplitude surface roughness parameters according to ISO 4287 in relation to the average values for each tool wear condition.

As shown in Table 8, in general, only the material ratio parameters of the workpiece surface resulted in overall good correlations with the roughness of the worn rake surface of the tool. In a similar way, only the functional (volume) and hybrid parameters of the rake surface resulted in good correlation with the surface roughness of the workpiece. The generally inverse correlation between the *Rmr* of the workpiece and the roughness parameters of the rake face can be explained by the fact that the higher the cutting pressured caused by the increasing tool wear at the main cutting-edge also increasing the wear at the rake face. This higher wear results in a more unstable chip flow and leads to poorer roughness at the machined surface, what in turn leads to lower material ratio at c = 1 µm under the highest peak, as the plastic deformation is favoured in relation to the pure shearing process. The *Rdc* behaves inversely as it is more correlated with the bulk of the profile (height difference between 20% and 80% of material ratios).

The *Rdq* parameter of the spacing class also resulted in relatively good correlations with the roughness of the rake face of the tool as the tool wear increases, (79.3%), indicating that the changes in the slope of the workpiece roughness profile are directly correlated with the increased wear at the rake face. In a similar way of the results found for the amplitude parameters (Table 7) of the workpiece roughness profile, the hybrid and functional volume parameters of the worn rake face also resulted in the better correlations as the wear at the main cutting edge increases.

4 I CONCLUSIONS

In this paper was discussed a novel approach to correlate the roughness parameters of the worn rake face of cemented carbide cutting tools with the resulting surface roughness of the workpiece, under different cutting atmospheres, machining parameters and tool wears (VBB). The following conclusions could be drawn in relation to the correlations:

- In relation to the input variables the overall highest correlations between the rake face and workpiece roughness were found for the average values for the cutting parameters.
- The best class of parameter for modelling the roughness of the workpiece was the Functional (volume) of the roughness at the worn surface of the tool, as it averaged more than 80% correlation between the input variables with no average lower than 70%.
- The best class of parameter for modelling the roughness at the worn surface of the tool was the amplitude parameter of the workpiece surface roughness.

ACKNOWLEDGEMENTS

The authors are grateful to the Brazilian research agencies CNPq, FAPEMIG and Coordenação de Aperfeiçoamento de Pessoal de Nível Superior - Brasil (CAPES) - Finance Code 001 financial support. The auhors are also gratefull for Pontifícia Universidade Católica do Paraná – PUCPR do Brazil and the Federal University of Uberlândia for the technical support.

REFERENCES

1 POPPER, K. Philosophy of science. **British Philosophy in the Mid-Century (ed. CA Mace). London: George Allen and Unwin**, 1957.

2 MACHADO, Á. R.; DINIZ, A. E. Tool wear analysis in the machining of hardened steels. **The International Journal of Advanced Manufacturing Technology,** v. 92, n. 9, p. 4095-4109, 2017/10/01 2017. ISSN 1433-3015. Disponível em: < https://doi.org/10.1007/s00170-017-0455-2 >.

3 DEVILLEZ, A.; LESKO, S.; MOZER, W. Cutting tool crater wear measurement with white light interferometry. **Wear,** v. 256, n. 1, p. 56-65, 2004/01/01/ 2004. ISSN 0043-1648. Disponível em: < http://www.sciencedirect.com/science/article/pii/S0043164803003843 >.

4 DA SILVA, L. et al. Critical assessment of compacted graphite cast iron machinability in the milling process. **Journal of Manufacturing Processes,** v. 56, p. 63-74, 2020. ISSN 1526-6125.

5 FAVERO FILHO, A. et al. Influence of milling direction in the machinability of Inconel 718 with submicron grain cemented carbide tools. **The International Journal of Advanced Manufacturing Technology,** v. 105, n. 1-4, p. 1343-1355, 2019. ISSN 0268-3768.

6 DOLINŠEK, S.; KOPAČ, J. Acoustic emission signals for tool wear identification. **Wear,** v. 225-229, p. 295-303, 1999/04/01/ 1999. ISSN 0043-1648. Disponível em: < http://www.sciencedirect.com/science/article/pii/S0043164898003639 >.

7 BONIFACIO, M. E. R.; DINIZ, A. E. Correlating tool wear, tool life, surface roughness and tool vibration in finish turning with coated carbide tools. **Wear,** v. 173, n. 1, p. 137-144, 1994/04/01/ 1994. ISSN 0043-1648. Disponível em: < http://www.sciencedirect.com/science/article/pii/0043164894902666 >.

8 DA SILVA, L. R. R. et al. Tool Wear Monitoring in Drilling of High Strength CGIs. **ImechE – Part B Journal of Engineering Manufacture**, 2020.

9 ASTAKHOV, V. P. **Tribology of metal cutting**.   Elsevier, 2006. ISBN 0080466850.

10 ISO-3685. Tool-life testing with single-point turning tools. 1993.

11 ISO-8688. **Tool life testing in milling** 1989.

12 CHOU, Y. K.; EVANS, C. J. Tool wear mechanism in continuous cutting of hardened tool steels. **Wear,** v. 212, n. 1, p. 59-65, 1997/11/30/ 1997. ISSN 0043-1648. Disponível em: < http://www.sciencedirect.com/science/article/pii/S0043164897001397 >.

13 SAYIT, E.; ASLANTAS, K.; ÇIÇEK, A. Tool wear mechanism in interrupted cutting conditions. **Materials and Manufacturing Processes,** v. 24, n. 4, p. 476-483, 2009. ISSN 1042-6914.

14 DOS SANTOS, A. G.; DA SILVA, M. B.; JACKSON, M. J. Tungsten carbide micro-tool wear when micro milling UNS S32205 duplex stainless steel. **Wear,** v. 414-415, p. 109-117, 2018/11/15/ 2018. ISSN 0043-1648. Disponível em: < http://www.sciencedirect.com/science/article/pii/S004316481730580X >.

15 CARVALHO, D. O. A. et al. Performance evaluation of vegetable-based cutting fluids in turning of AISI 1050 steel. **The International Journal of Advanced Manufacturing Technology**, p. 1-17, 2019. ISSN 0268-3768.

16 YOVANOVICH, M. Micro and Macro Hardness Measurements, Correlations, and Contact Models. **Collection of Technical Papers - 44th AIAA Aerospace Sciences Meeting,** v. 16, 01/09 2006.

17 SILVA, L. R. R. et al. Analysis of the coefficient of friction at the workpiece-tool interface in milling of high strength compacted graphite cast irons. **Wear,** v. 426-427, n. April, p. 1646-1657, 2019 2019. ISSN 00431648.

18 ISO, I. 25178-2: 2012—Geometrical Product Specifications (GPS)—Surface Texture: Areal—Part 2: Terms, Definitions and Surface Texture Parameters. **International Standards Organization: Geneva, Switzerland**, 2012.

19 ISO, E. 4287–Geometrical Product Specifications (GPS)–Surface Texture: Profile Method–Terms, Definitions and Surface Texture Parameters. **International Organization for Standardization: Geneva, Switzerland**, 1997.

20 DA SILVA, A. E. et al. Relationship between mechanical and metallurgical properties with machinability when drilling high-strength cast irons. **The International Journal of Advanced Manufacturing Technology,** v. 106, n. 7-8, p. 3389-3407, 2020. ISSN 0268-3768.

21 MUSFIRAH, A. H.; GHANI, J. A.; HARON, C. H. C. Tool wear and surface integrity of inconel 718 in dry and cryogenic coolant at high cutting speed. **Wear,** v. 376-377, p. 125-133, 2017/04/15/ 2017. ISSN 0043-1648. Disponível em: < http://www.sciencedirect.com/science/article/pii/S0043164817301060 >.

22 HADDAG, B.; NOUARI, M. Tool wear and heat transfer analyses in dry machining based on multi-steps numerical modelling and experimental validation. **Wear,** v. 302, n. 1, p. 1158-1170, 2013/04/01/ 2013. ISSN 0043-1648. Disponível em: < http://www.sciencedirect.com/science/article/pii/S0043164813000483 >.

ÍNDICE REMISSIVO

V

Engenharia Mecânica:
Inovações Tecnológicas de Elevado Valor

www.atenaeditora.com.br
contato@atenaeditora.com.br
@atenaeditora
www.facebook.com/atenaeditora.com.br

Atena Editora
Ano 2021

Engenharia Mecânica:
Inovações Tecnológicas de Elevado Valor

www.atenaeditora.com.br
contato@atenaeditora.com.br
@atenaeditora
www.facebook.com/atenaeditora.com.br

Atena Editora
Ano 2021